IBRO Neuroscience Reports 18 (2025) 539–544

Contents lists available at ScienceDirect

IBRO Neuroscience Reports

journal homepage: www.sciencedirect.com/journal/IBRO-Neuroscience-Reports

Parvalbumin-positive primary afferent projections to motoneurons increase after complete spinal transection in neonatal and juvenile rats

Masahito Takiguchi [a], Ryutaro Matsuyama [a], Satoru Shinoda [b], Kengo Funakoshi [a,*]

[a] Department of Neuroanatomy, Yokohama City University School of Medicine, Kanazawa-ku, Yokohama, Japan
[b] Department of Biostatics, Yokohama City University School of Medicine, Kanazawa-ku, Yokohama, Japan

ARTICLE INFO

Keywords:
Spinal cord injury
Neonate
Juvenile
Parvalbumin
Primary afferents
Motoneurons

ABSTRACT

Hindlimb locomotor activity spontaneously recovers after complete spinal cord transection (CST) in neonatal rats, but not in juvenile rats. A previous study in neonatal rats that underwent CST at the thoracic level demonstrated that primary afferent projections increase in the ventral horn and intermediate zone at the lumbar level. It remains unclear whether primary afferent terminals of motoneurons increase and whether primary afferent projections to the spinal cord are altered after CST in juvenile rats. Here, we used biotinylated dextran amine as a tracer to demonstrate that primary afferent projections to the ventral horn and intermediate zone were significantly increased in rats that underwent CST in the juvenile period compared to intact rats of the same age. We then examined Ia afferents using immunohistochemistry for parvalbumin. Our findings revealed an increase in parvalbumin-immunoreactive terminals on motoneurons in both neonatal and juvenile rats after CST compared to intact rats of the same age. These results suggest that proprioceptive afferent terminals on motoneurons are increased after CST in both neonatal and juvenile rats. In neonatal rats, this increase might contribute to the spontaneous recovery of hindlimb motor activity after CST, whereas in juvenile rats, the increase in proprioceptive afferent terminals on motoneurons does not contribute to recovery following CST.

1. Introduction

Spinal cord injury in adults may cause sensorimotor and autonomic dysfunction leading to death (Krassioukov et al., 2007). Complete spinal cord transection (CST) at the thoracic level in adult and juvenile rats produces permanent loss of hindlimb locomotor function. Neonatal rats, however, spontaneously recover hindlimb locomotor activity after CST (Stelzner et al., 1975; Yuan et al., 2013). The critical period for this functional recovery is 10–15 days of age (Yuan et al., 2013; Takiguchi et al., 2015, 2022).

The mechanisms underlying the spontaneous recovery in neonatal rats are poorly understood. A previous study in which the anterograde tracer biotinylated dextran amine (BDA) was administered into the dorsal root ganglion (DRG) in neonatal rats after CST at the thoracic level reported enhanced primary afferent projections to the lumbar spinal motor area, such as the intermediate zone and ventral horn (Takiguchi et al., 2015, 2018). This plasticity of the primary afferents in neonatal rats might be involved in the successful recovery of locomotor function because axonal regeneration of descending tracts through the injury is not observed after CST during the neonatal period (Tillakaratne et al., 2010; Takiguchi et al., 2015). Whether primary afferent terminals on motoneurons in the ventral horn increase after CST and which categories of primary afferents contribute to increased projections to motoneurons, however, remains unclear. It is also unknown whether primary afferent projections to the lumber motor area are altered in juvenile rats that undergo CST, in which spontaneous recovery of hindlimb motor activity does not occur.

In this study, therefore, we first injected BDA into the fifth lumbar dorsal root ganglion (L5 DRG) of rats that underwent CST at postnatal day (P) 20, i.e., during the juvenile period, and quantitatively examined the primary afferent fibers and their terminals in the spinal motor area of the L5 spinal segment. We next quantitatively examined parvalbumin-positive nerve terminals on motoneurons in the L5 spinal segment of rats that underwent CST at P5 and P20. Parvalbumin is expressed specifically in the Ia afferents that transmit proprioceptive sensory information from muscle spindles (Carr et al., 1989; Prasad and Weiner, 2011; Wang et al., 2017). Motoneurons were identified as neurons immunoreactive for choline acetyltransferase (ChAT) in the ventral horn (Barber et al., 1984). Our findings revealed that the number of parvalbumin-positive Ia afferent terminals on motoneurons increased

* Correspondence to: Department of Neuroanatomy, Yokohama City University School of Medicine, 3-9 Fukuura, Kanazawa-ku, Yokohama 236-0004, Japan
E-mail address: funako@yokohama-cu.ac.jp (K. Funakoshi).

https://doi.org/10.1016/j.ibneur.2025.03.011
Received 25 October 2024; Received in revised form 29 March 2025; Accepted 29 March 2025
Available online 1 April 2025

after CST in rats at P5 and P20, suggesting that proprioceptive Ia afferent projections to motoneurons were enhanced after CST regardless of the rats' age at injury. Other factors, therefore, might be responsible for the different motor recovery outcomes after CST between neonatal and juvenile rats.

2. Materials and methods

2.1. Materials

Wistar neonatal and juvenile rats of both sexes (n = 23, Japan SLC, Hamamatsu, Japan) and their dams were used in the present study. All experimental procedures were performed according to the standards established by the NIH Health Guide for the Care and Use of Laboratory Animals and the Policies on the Use of Animals and Humans in Research. The protocols were approved by the Institutional Animal Care and Use Committee of the Animal Research Center, Yokohama City University Graduate School of Medicine (approval nos. F19–004 and F-A-22–058).

2.2. Complete spinal cord transection

Spinal cords of neonatal rats (P5, n = 5) or juvenile rats (P20, n = 7) were transected at the 10th thoracic level (T10) as previously described (Takiguchi et al., 2015). Under isoflurane gas (1.5 %–2.0 %) anesthesia, spinal cords were completely transected with small spring microscissors following partial laminectomy (T9-T10). After confirming that the spinal transection was complete, bleeding was stopped with Spongel (LTL Pharma Co., Ltd., Tokyo, Japan). The muscles, fascia, and skin were closed in layers with 5–0 nylon sutures. Upon recovering from the anesthesia, all rats were gently cleaned with gauze soaked in 70 % ethanol to eliminate the smell of blood and returned to their home cages. All rats with CST were housed individually in polycarbonate cages in a room maintained at 25 ± 1°C, with a 07:00 on/19:00 off light cycle.

2.3. Administration of anterograde tracer into the DRG

To label the primary afferent fibers, BDA (MW 10,000, D1956, Life Technologies, Carlsbad, CA, USA), an anterograde tracer, was used. At P33, rats that received spinal transection at P20 (P20ST rats, n = 3) and intact rats (n = 3) were anesthetized with isoflurane gas as described above, and the left DRGs of the L5 nerves were exposed by unilateral laminectomy. BDA (0.5 μL; 10 % in distilled water) was injected into the DRGs using a glass pipette attached to a manipulator (MNM-333, Narishige, Tokyo, Japan). The tip of the pipette was 50 μm in diameter, and the pipette was connected to a 1.0-μL Hamilton syringe by polyethylene tubing (size 5, Igarashi Ika Kogyo Co., Ltd., Tokyo, Japan).

2.4. Tissue preparation for BDA histochemistry

One week after BDA administration, P20ST rats and intact rats were deeply anesthetized with isoflurane gas and transcardially perfused with normal saline followed by 4 % paraformaldehyde (PFA) in 0.1 M phosphate buffer. The spinal cord was dissected and postfixed with 4 % PFA overnight at 4°C.

2.5. BDA histochemistry

BDA was visualized as previously described (Takiguchi et al., 2015), using a Vectastain Elite ABC standard kit (PK-6100, Vector Laboratories, Inc., Burlingame, CA, USA) according to the manufacturer's protocol. After several washes in phosphate-buffered saline (PBS), free-floating sections were incubated in 0.3 % H_2O_2 in methanol for 30 min at room temperature. The sections were then incubated in a mixture of Solution A and B from the kit and Triton X-100. After rinsing in PBS and Tris-buffered saline (TBS, pH 7.4), the sections were incubated in diaminobenzidine-Ni reaction solution containing 0.01 % diaminobenzidine, 1.0 % nickel ammonium sulfate, and 0.0003 % H_2O_2 in TBS for 30 min. After several washes in TBS, the sections were placed on gelatin-coated slide glasses, dried, and dehydrated in an ascending series of ethanol (50 %, 70 %, 90 %, 95 %, 3_X99 %) followed by xylene three times, and then coverslipped.

2.6. Fixation and tissue preparation for immunohistochemistry

At 2 weeks after CST, the P5ST (n = 5) and P20ST rats (n = 4) were deeply anesthetized with isoflurane, and transcardially perfused with normal saline followed by 4 % PFA in 0.1 M phosphate buffer. Intact rats at P19 (n = 4) and P34 (n = 4) were perfused in the same manner. The spinal cords were dissected and postfixed with 4 % PFA overnight at 4°C. The tissues were then cryoprotected in 30 % sucrose for 2 days and embedded in OCT compound via 2-methylbutane (isopentane) in liquid N_2. Sections of the spinal cord at the lumbar level from P5ST rats, P20ST rats, P19 intact rats, and P34 intact rats were serially cut at 20 μm with a cryostat (CM3050 S, Leica, Nussloch, Germany). Serial Sections (1 in 5) were collected, and 5 series of sections were prepared.

2.7. Immunohistochemistry

A series of sections were incubated in a moist chamber overnight at 4°C with a mixture of goat polyclonal IgG antibody against ChAT (1:100; AB144P, Merck KGaA, Darmstadt, Germany) and rabbit polyclonal antibody against parvalbumin (1:200; Synaptic Systems, Göttingen, Germany), diluted with 1 % normal donkey serum, 0.2 % bovine serum albumin, and 0.1 % NaN_3 in 0.025 M PBS with Tween 20 (PBST). The sections were rinsed several times with 0.025 M PBST and then incubated for 2 h at room temperature with a mixture of secondary antibodies: Alexa Fluor 488-conjugated donkey anti-rabbit IgG (10 μg/ml; Jackson ImmunoResearch Laboratories, West Grove, PA, USA) and cyanine Cy3-conjugated donkey anti-goat IgG (10 μg/ml; Jackson ImmunoResearch Laboratories).

Another series of sections of P20ST rats was incubated with a mixture of goat polyclonal IgG antibody against ChAT (1:100; Merck KGaA), rabbit polyclonal antibody against parvalbumin (1:200; Synaptic System), and mouse monoclonal antibody against synapsin I (1:200; VAM-SV009, StressGen Biotechnologies Corp., San Diego, CA, USA). The sections were rinsed several times with 0.025 M PBST and then incubated for 2 h at room temperature with a mixture of secondary antibodies: Alexa Fluor 647-conjugated donkey anti-rabbit IgG (10 μg/ml; Jackson ImmunoResearch Laboratories), cyanine Cy3-conjugated donkey anti-goat IgG (10 μg/ml; Jackson ImmunoResearch Laboratories), and Alexa Fluor 488-conjugated donkey anti-mouse IgG (10 μg/ml; Jackson ImmunoResearch Laboratories).

The antibody specificity was verified by incubating the sections in 0.025 M PBST with 1 % normal donkey serum, 0.2 % bovine serum albumin, and 0.1 % NaN_3 instead of the primary antibodies. The slides were rinsed five times with PBS, and coverslipped with slow-fade reagent (SlowFade Diamond Antifade Mountant, S36936, Life Technologies Corporation).

2.8. Image acquisition and analysis

All the spinal sections at the fifth lumbar level were digitally photographed through a 10x or 20x objective using a Keyence BIOREVO microscope (BZ-9000, Keyence, Osaka, Japan) and transferred to Adobe Photoshop CS (Adobe, San Jose, CA, USA). Final magnification was confirmed by inserting a stage micrometer into the microscope and measuring the captured scale on the Photoshop screen. The triple-labeled images were converted to pseudocolor to facilitate visualization. The contrast and brightness were adjusted using Adobe Photoshop Software.

The number of terminal buttons and the axonal length of BDA-positive fibers were analyzed as previously reported (Takiguchi et al.,

2015). Briefly, the spinal motor area was divided into the intermediate zone (IZ), lateral part of ventral horn (VHl), and medial part of ventral horn (VHm), and the number of terminal buttons in each section (3 sections per animal) was counted in a blinded manner. The values were averaged for all animals in each group and are expressed as the mean number ± standard error of the mean (SEM). The length of BDA-positive fibers in the same region of each section was automatically measured using BZ-analyzer software (Keyence). A Student's *t*-test was used to compare the mean values between two groups. *p*-values of less than 0.05 were considered significant in a two-tailed test.

For immunohistochemistry, the number of parvalbumin-positive nerve terminals on ChAT-positive neurons in the ventral horn of each section (1.5–2 sections per animal) was counted in a blinded manner. The mean number of terminals on neurons was calculated per section and per neuron for each animal, averaged for all animals in each group, and are expressed as mean ± SEM. Statistical analysis was performed by a two-way analysis of variance (ANOVA) using SPSS software (IBM, Armonk, NY, USA), which employs the sum-to-zero constraint. *p*-values of less than 0.05 were considered significant.

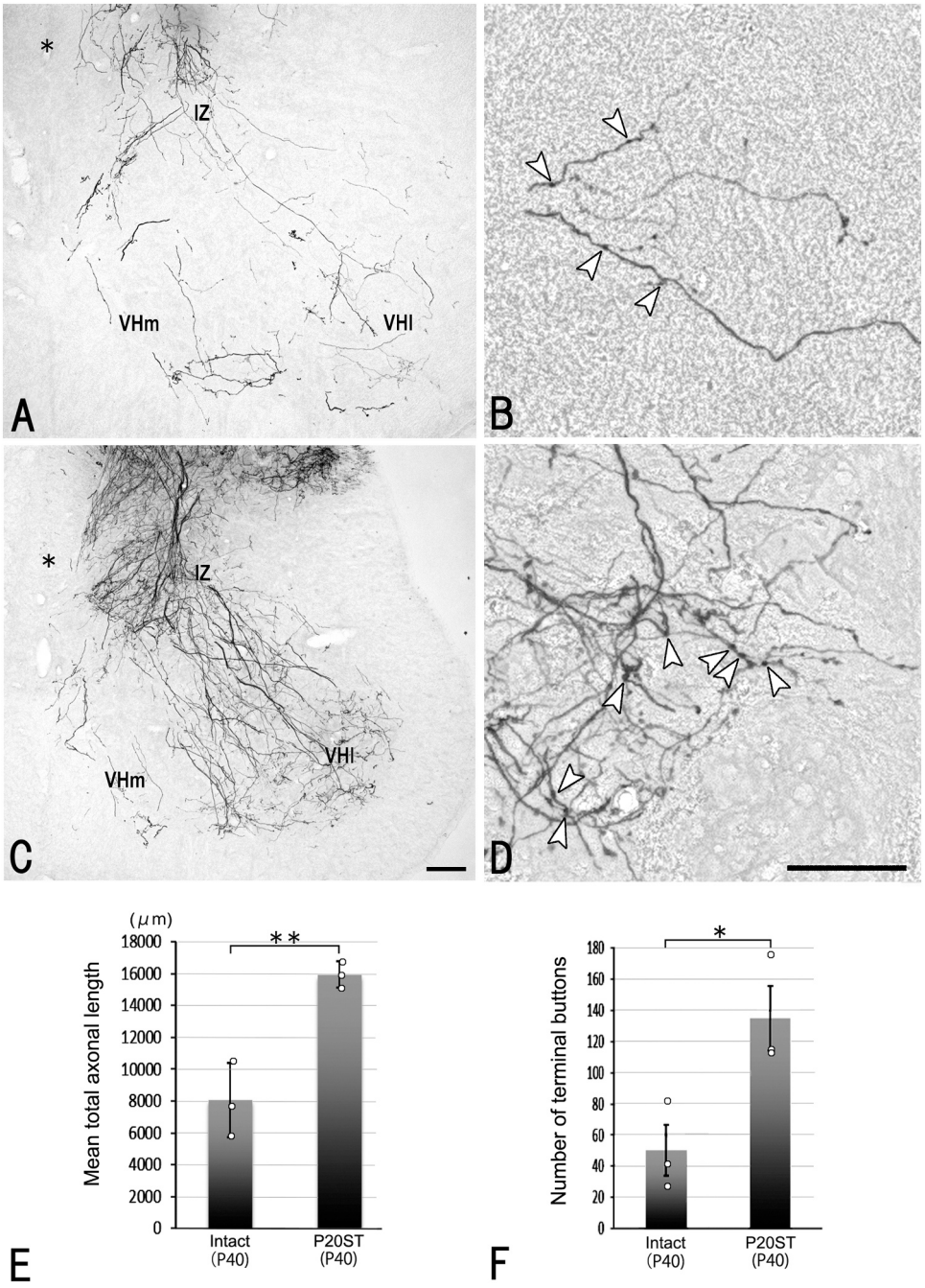

Fig. 1. Localization of BDA-labeled primary afferent fibers in the intermediate zone (IZ), lateral part of the ventral horn (VHl) and medial part of the ventral horn (VHm) of the L5 spinal cord. **A-D**: Images of intact rats at P40 (**A**, **B**) and P20ST rats at P40 (**C**, **D**). BDA was administered into the left DRG 1 week prior (P33) to perfusion. Arrowheads in **B** and **D** indicate terminal buttons. Asterisks: central canal. Scale bars: 100 μm in **C** (apply also to **A**), and 50 μm in **D** (apply also to **B**). **E**, **F**: Total axonal length (**E**) and the number of terminal buttons (**F**) of BDA-labeled fibers in the IZ, VHl, and VHm were significantly higher in P20ST rats than in intact rats. Data are expressed as mean ± SEM. Significant differences are indicated by * * ($p < 0.01$) or * ($p < 0.05$).

3. Results

3.1. BDA-labeled primary afferent fiber projection to L5 spinal cord

BDA-positive fibers were observed in the dorsal horn, IZ, VHl, and VHm on the ipsilateral side of L5 spinal segment (Fig. 1A and B). The total axonal length of BDA-positive fibers in the IZ, VHl, and VHm of P20ST rats was significantly longer than that of intact rats of the same age (P34 intact rats, Fig. 1C). The number of terminal buttons of BDA-positive fibers in the IZ, VHl, and VHm of P20ST rats was also significantly higher than that of intact rats of the same age (P34 intact rats, Fig. 1D).

The mean total axonal length of BDA-positive fibers of P20ST rats was 6346.4 μm in the IZ, 1160.6 μm in the VHm, and 8441.9 μm the VHl, whereas that in intact rats of the same age (P34 intact rats) was 3729.6 μm in the IZ, 595.4 μm in the VHm, and 3737.6 in the VHl. The mean total length (mean ± SEM) in all spinal motor areas was 15,948.9 ± 478.3 in P20ST rats and 8062.6 ± 1357.4 in P34 intact rats, with a *t*-test revealing a significant difference ($t(4) = 5.480$, $p = 0.0054$) between the mean values of the two groups (Fig. 1E). The mean number of terminal buttons of BDA-positive fibers of P20ST rats was 36.0 in the IZ, 20.6 in the VHm, and 78.1 in the VHl, whereas that in intact rats of the same age (P34 intact rats) was 18.2 in the IZ, 13.6 in the VHm, and 18.3 in the VHl. The mean number of terminal buttons (mean ± SEM) in all spinal motor areas was 134.7 ± 20.7 in P20ST rats and 50.1 ± 16.3 in P34 intact rats, with a *t*-test revealing a significant difference ($t(4) = 3.209$, $p = 0.0326$) between the mean values of the two groups (Fig. 1F).

3.2. Parvalbumin-positive nerve terminals on ChAT-immunoreactive motoneurons

Numerous parvalbumin-positive nerve fibers were observed in the intermediate zone and ventral horn. Additionally, many parvalbumin-positive nerve terminals were observed on the cell bodies of ChAT-immunoreactive neurons in the ventral horn (Figs. 2, 3A-D). All of the parvalbumin nerve terminals on the ChAT-immunoreactive neurons in P20ST rats were also positive for synapsin I, a major presynaptic marker (Fig. 3E, F). The mean number of parvalbumin-positive nerve terminals on ChAT-immunoreactive neurons was 61.3 ± 8.8 per section 2 weeks after CST in P20ST rats and 38.1 ± 5.5 per section in intact rats of the same age (P19 intact rats). The mean number of parvalbumin-positive nerve terminals on ChAT-immunoreactive neurons was 53.3 ± 7.3 per section 2 weeks after CST in P20ST rats and 16.8 ± 2.4 per section in intact rats of the same age (P34 intact rats, Fig. 3G). Statistical analysis using two-way ANOVA revealed a significant difference ($F(1,13) = 18.517$, $p = 0.001$) between the groups treated with and without CST, but no significant difference ($F(1,13) = 4.478$, $p = 0.054$) was found between ages (P19 vs. P34). There was no interaction between CST treatment and age ($F(1,13) = 0.933$, $p = 0.352$).

The mean number of parvalbumin-positive nerve terminals on ChAT-immunoreactive neurons was 3.19 ± 0.38 per neuron 2 weeks after CST in P5ST rats and 1.72 ± 0.27 per neuron in intact rats of the same age (P19 intact rats). The mean number of parvalbumin-positive nerve terminals on ChAT-immunoreactive neurons was 3.34 ± 0.31 per neuron 2 weeks after CST in P20ST rats and 1.14 ± 0.16 per neuron of intact rats of the same age (P34 intact rats, Fig. 3H). Statistical analysis using two-way ANOVA revealed a significant difference ($F(1,13) = 35.032$, $p < 0.001$) between the groups treated with and without CST, but no significant difference ($F(1,13) = 0.480$, $p = 0.500$) was found between ages (P19 vs. P34). There was no interaction between CST treatment and age ($F(1,13) = 1.410$, $p = 0.256$).

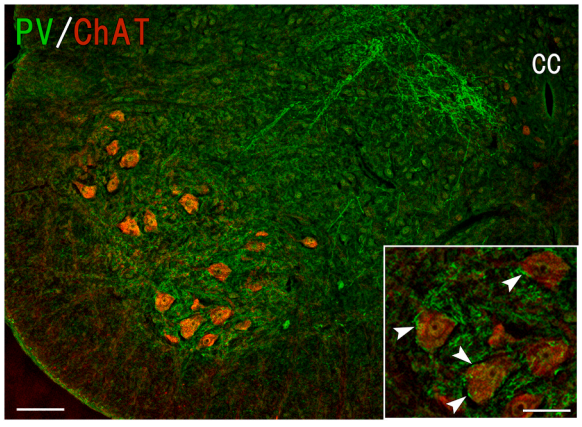

Fig. 2. Representative parvalbumin-immunoreactivity in the L5 spinal cord of a P5ST rat. Parvalbumin-immunoreactive fibers (green) were observed in the IZ, and around ChAT-positive motoneurons (red) in the ventral horn. Inset: a higher magnification image of parvalbumin-immunoreactive terminals (arrowheads) on ChAT-positive motoneurons. CC: central canal. Scale bars: 100 μm, and 50 μm in the inset.

4. Discussion

Hindlimb motor function in rats with CST during the neonatal period is considerably recovered at 2 weeks after CST as assessed by the Basso, Beattie, and Bresnahan scale, although forelimb coordination was not observed (Tillakaratne et al., 2010, Takiguchi et al., 2015, 2022). A previous study in which BDA was injected into the DRGs demonstrated that the axonal length and number of terminal buttons of primary afferents in P5ST rats in the L5 ventral horn was significantly higher than that in intact rats at the same age (P19 intact rats), which suggested that an increase in primary afferent projections to the spinal motor area induced locomotor recovery after CST during the neonatal period (Takiguchi et al., 2015). The present study revealed that the number of parvalbumin-positive nerve terminals on ChAT-positive neurons in the P5ST rats was significantly higher than that in intact rats at the same age (P19 intact rats), suggesting that the proprioceptive afferent projections to the motoneurons were enhanced by the CST. The present study, therefore, provides further insight into the mechanisms of motor recovery after CST during the neonatal period. In the present study, parvalbumin-positive neurons were observed in the ventral horn and intermediate zone in the CST groups and intact rats. These neurons were assumed to be Ia inhibitory interneurons or Renshaw cells (Celio, 1990), now included among V1 and V2b interneurons of the central patter generator (Grillner and Kozlov, 2021). Some of the parvalbumin-positive nerve terminals on ChAT-positive neurons, which increase following CST, therefore, might be derived from inhibitory interneurons, but not from Ia afferents. Changes in inhibitory inputs to motoneurons might also be related to motor function recovery following CST.

The present study also revealed that the total axonal length and the number of terminal buttons of BDA-positive primary afferent fibers in the L5 ventral horn of P20ST rats was significantly higher than that in intact rats at the same age (P34 intact rats). Furthermore, the number of parvalbumin-positive nerve terminals on ChAT-positive neurons in P20ST rats was significantly higher than that in intact rats at the same age (P34 intact rats) and rats transected at nearly the same time (P19 intact rats). These findings suggest that both the primary afferent projections to the spinal cord and proprioceptive afferent contacts to the motoneurons were enhanced following CST during the juvenile period, after which motor recovery is poor. Thus, although CST performed during the juvenile period might induce remodeling of compensatory neural connections, the remodeling does not induce the recovery of locomotor activity. Thes present results, therefore, suggest that the increased afferent projections to motoneurons after SCT in neonatal rats and juvenile rats are independent of the recovery of motor activity, but differences in synaptic plasticity affecting the remodeling of neural connections between neonatal and juvenile rats might be related to the

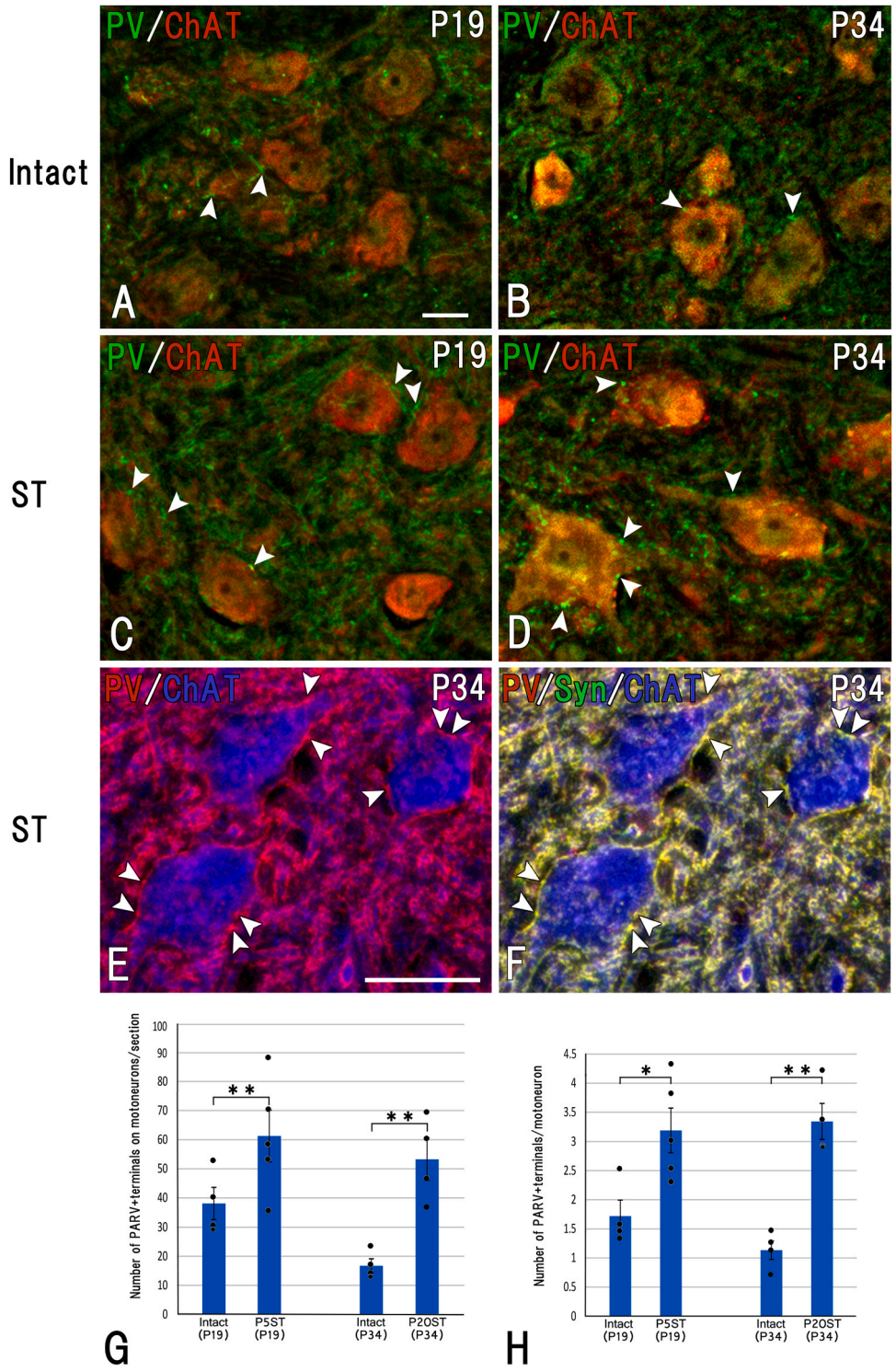

Fig. 3. Parvalbumin-immunoreactive nerve terminals on ChAT-immunoreactive neurons in the L5 ventral horn. **A**, **B**: Images of an intact rat at P19 (**A**), and P34 rats (**B**). **C**, **D**: Images of a rat with CST at P5 (P5ST rats, **C**), and P20 (P20ST rats, **D**). Arrowheads indicate parvalbumin-nerve terminals on ChAT-immunoreactive neurons. **E**, **F**: Triple labeling of parvalbumin (red), ChAT (blue), and synapsin I (green). The parvalbumin-immunoreactive nerve terminals (arrowheads in **E**) on ChAT-positive neurons were also positive for synapsin I (arrowheads in **F**). Scale bars: 50 μm in **A** (applies also to **B**-**D**), and 50 μm in **E** (apply also to **F**). **G, H**: Number of parvalbumin-immunoreactive terminals on ChAT-immunoreactive neurons per section (**G**) and per neuron (**H**). Data are expressed as mean ± SEM. Dots indicate individual data points. Significant differences are indicated by * * ($p < 0.01$) or * ($p < 0.05$).

differences observed in their motor recovery.

Perineuronal nets (PNNs) are reticular structures surrounding neuronal cell bodies in the central nervous system. The formation of PNNs is related to the establishment of synaptic connections during the developmental process and is considered to coincide with closure of the critical period for synaptic plasticity (Kwok et al., 2011, Wang and Fawcett, 2012). In intact rats, PNN formation around motoneurons at the lumbar level increases rapidly after P20, reaching about half the total by P35 (Takiguchi et al., 2021). A previous study suggested that the PNN formation around motoneurons in the L5 spinal segment is

suppressed after CST during the neonatal period, and that the decrease in PNNs might facilitate the formation of new synaptic contacts to motoneurons (Takiguchi et al., 2022). The reduction of PNNs, therefore, might be associated with an increase in parvalbumin-positive proprioceptive primary afferents terminals on motoneurons and thus with the recovery of locomotor activity in rats with CST during the neonatal period.

Takiguchi et al. (2022) revealed that PNN formation around motoneurons at the lumbar level was slightly upregulated by CST during the juvenile period. The PNNs around motoneurons expressed after closure of the critical period might inhibit new synapse formation, and thus a significant number of primary afferents newly induced by CST during the juvenile period might have been prevented by PNNs from contacting the appropriate targets of motoneurons. The increased parvalbumin-positive proprioceptive primary afferent terminals on inappropriate motoneurons might lead to poor recovery of locomotor activity in juvenile rats after CST.

Ethical statement

This study was carried out in accordance with the recommendations of The Yokohama City University Committee for Animal Research. The project was approved by The Yokohama City University Committee for Animal Research (approval nos. F19–004 and F-A-22–058). All procedures were performed according to the standards established by the NIH Guide for the Care and Use of Laboratory Animals and the Policies on the Use of Animals and Humans in Research. All efforts were made to minimize the number of animals used and their suffering.

CRediT authorship contribution statement

Funakoshi Kengo: Writing – review & editing, Supervision, Project administration, Funding acquisition, Conceptualization. **Shinoda Satoru:** Data curation. **Matsuyama Ryutaro:** Visualization, Investigation, Formal analysis. **Takiguchi Masahito:** Visualization, Validation, Resources, Methodology, Investigation, Formal analysis, Data curation.

Declaration of Competing Interest

The authors declare that they have no known competing financial interests or personal relationships that could have appeared to influence the work reported in this paper.

Acknowledgements

We are grateful to Dr. K. Imura, Dr. A. Takeda, Dr. M. Yanagi, Dr. Y. Ikeda, Dr. K. Katsuki, and Mrs. M. Kobayashi for their expert advice. This work was supported in part by Grant-in-Aid #19K06927 from the Japan Society for the Promotion of Science. We also thank SciTechEdit International LLC (Highlands Ranch, CO, USA) for editing support.

Data Availability

Data available on request from the authors.

References

Barber, R.P., Phelps, P.E., Houser, C.R., Crawford, G.D., Salvaterra, P.M., Vaughn, J.E., 1984. The morphology and distribution of neurons containing choline acetyltransferase in the adult rat spinal cord: an immunocytochemical study. J. Comp. Neurol. 229, 329–346.

Carr, P.A., Yamamoto, T., Karmy, G., Baimbridge, K.G., Nagy, J.I., 1989. Parvalbumin is highly colocalized with calbindin D28k and rarely with calcitonin gene-related peptide in dorsal root ganglia neurons of rat. Brain Res 497, 163–170.

Celio, M.R., 1990. Calbindin D-28k and parvalbumin in the rat nervous system. Neuroscience 35, 375–475.

Grillner, S., Kozlov, A., 2021. The CPGs for limbed locomotion-facts and fiction. Int. J. Mol. Sci. 22, 5882.

Krassioukov, A.V., Karlsson, A.K., Wecht, J.W., Wuermser, L.A., Mathias, C.J., Marino, R. J., 2007. Assessment of autonomic dysfunction following spinal cord injury: rationale for additions to International Standards for Neurological Assessment. J. Rehabil. Res. Dev. 44, 103–112.

Kwok, J.C.F., Dick, G., Fawcett, J.W., 2011. Extracellular matrix and perineuronal nets in CNS repair. Dev. Neurobiol. 71, 1073–1089.

Prasad, T., Weiner, J.A., 2011. Direct and indirect regulation of spinal cord Ia afferent terminal formation by the γ-protocadherins. Front. Mol. Neurosci. 4, 54.

Stelzner, D.J., Ershler, W.B., Weber, E.D., 1975. Effects of spinal transection in neonatal and weanling rats: survival of function. Exp. Neurol. 46, 156–177.

Takiguchi, M., Atobe, Y., Kadota, T., Funakoshi, K., 2015. Compensatory projections of primary sensory fibers in lumbar spinal cord after neonatal thoracic spinal transection in rats. Neuroscience 304, 349–354.

Takiguchi, M., Fujioka, M., Funakoshi, K., 2018. Neonatal spinal injury induces de novo projections of primary afferents to the lumbosacral intermediolateral nucleus in rats. IBRO Rep. 4, 1–6.

Takiguchi, M., Morinobu, S., Funakoshi, K., 2021. Chondroitin sulfate expression around spinal motoneurons during postnatal development in rats. Brain Res 1752, 147252.

Takiguchi, M., Akaike, T., Shindo, K., Sakuyama, R., Koganemaru, R., Funakoshi, K., 2022. Chondroitin sulfate expression around motoneurons changes after complete spinal transection of neonatal rats. Neurosci. Lett. 766, 136324.

Tillakaratne, N.J.K., Guu, J.J., de Leon, R.D., Bigbee, A.J., London, N.J., Zhong, H., Ziegler, M.D., Joynes, R.L., Roy, R.R., Edgerton, V.R., 2010. Functional recovery of stepping in rats after a complete neonatal spinal cord transection is not due to regrowth across the lesion site. Neuroscience 166, 23–33.

Yuan, Q., Su, H., Chiu, K., Wu, W., Lin, Z., 2013. Contrasting neuropathology and functional recovery after spinal cord injury in developing and adult rats. Neurosci. Bull. 29, 509–516.

Wang, D., Fawcett, J., 2012. The perineuronal net and the control of CNS plasticity. Cell Tissue Res 349, 147–160.

Wang, L., Yu, C., Wang, J., Zhao, H., Chan, S.O., 2017. The spatiotemporal relationships between chondroitin sulfate proteoglycans and terminations of calcitonin gene related peptide and parvalbumin immunoreactive afferents in the spinal cord of mouse embryos. Neurosci. Lett. 655, 61–67.